

# An Analysis of the Impact on Frequency Response with Penetration of RES in Power System and Modified Virtual Inertia Controller

H. Nerkar\*, P. Kundu, A. Chowdhury

Electrical Engineering Department, Sardar Vallabhbhai National Institute of Technology Surat, Gujarat, India.

**Abstract** - The power system in upcoming years will face issues of power frequency instability due to an increase in the share of Renewable Energy Sources (RES). The RESs are integrated into the power system through the power electronic converters. The operation and control of RES are drastically different than the conventional energy sources. This paper is focused on the effect of a rise in the share of RES on power system frequency stability and its possible solutions. The RESs are not taking part in the frequency regulation process in case of disturbance. Despite this, they generate disturbances in the power system caused by the intermittent nature of input energy. The RES doesn't have extra active power for the frequency regulation as they already operate at their maximum power point. These power electronic-based generators don't contain inertia like conventional generators. The inertia-less systems adversely affect the Rate of Change of Frequency (RoCoF) and frequency nadir. This is demonstrated on IEEE 9-bus system with different scenarios. According to that analysis, the RES should provide an inertial response during disturbances. In this paper, the proposed Modified Virtual Inertia Control (M-VIC) technique emulates inertia like conventional generators by using external Energy Storage Systems (ESS). In M-VIC the inertial response is replicated by controlling the rate and duration of power provided by ESS. The proposed technique is more effective to reduce the frequency nadir and RoCoF with better utilization of ESS. To demonstrate this, the PV integrated single-area power system model is simulated in MATLAB R2019a.

**Keyword:** Energy storage system, Frequency stability, Renewable energy sources, Rate of change of frequency, Virtual inertia control.

## 1. INTRODUCTION

The challenges of power system stability are increased by the rise in the share of Renewable Energy Sources in the existing power system. The higher percentage share of variable sources into the grid creates imbalances in generation and demand. The target of the Indian grid up to 2030 is to reach a 40% share of RES from total electricity generation. In total percentage of RES share, the contribution of solar and wind power is 45.2% and 36.7% respectively. The intermittent nature of RES threatens the reliable operation of the existing power system [1]. The existing power system contains a large share of synchronous generators, the resources are controlled and provide constant output. The input power of RES is neither constant nor controllable. The solar and wind power energy sources are integrated through the power electronic converters. The power electronic

converters are static devices and do not contain any rotating parts in the system. Due to this, the inertial response is absent in RES. The synchronous generators in conventional energy sources such as thermal, nuclear are electrically coupled with the grid. The low inertia systems cause frequency instability issues in the power system and might result in grid failure. The large contribution of RES to the power grid has a significant impact on the power system operation and stability. The inertial response is determined in seconds, and it can be implicated as the time required to release the kinetic energy stored (KE) in the rotor of a conventional generator. It can provide load equivalent to-rated apparent power of the conventional generator [2]. A power system inertia is characterized as the synchronous generator's capacity to oppose the change in frequency. Due to resistance is given by stored KE in the rotating masses of an individual turbine generator. The rotational inertia becomes a heterogeneous quantity as different areas have different inertia constant that depends on the share of RES [3]. The report of "entsoe (march 2016)" states the effect of decreased power system inertia will have a significant influence on the Continental European power system [4]. The Central Electricity

Received: 02 Sep. 2021

Revised: 06 Dec. 2021 and 31 Jan. 2022

Accepted: 18 Feb. 2022

\*Corresponding author:

E-mail: [harshadanerkar22@gmail.com](mailto:harshadanerkar22@gmail.com)

DOI: 10.22098/joape.2023.9494.1661

**Research Paper**

© 2023 University of Mohaghegh Ardabili. All rights reserved.

*Regularity Commission* (CERC) of India has addressed various measures to ameliorate the frequency profile in the Indian grid by progressively straining the frequency band. The tightening of the frequency band by CERC in subsequent emendations to Indian Electricity Grid Codes (IEGC) the frequency band with reference of 3<sup>rd</sup> May 2010 is 49.5 Hz to 50.2 Hz (i.e. -1% / +0.4%) [5]. In a report of ENTSO-E (2013) the network code for the requirement of grid connection mentions the synthetic inertia provided by the new generating unit should perform like a conventional system in grid operations [6]. In solar power generation, a limited amount of energy is stored in the DC link capacitor. This stored energy in DC-link capacitor can be used for providing virtual inertial power [7]. To provide virtual inertia in large solar PV plants when they operate at maximum power point the implicit option is an external ESS [8]. For imitating the inertia constant, the factors need to consider are RoCoF and Frequency nadir. The RoCoF is the parameter used for the protection of power system from the loss of synchronism [9]. There are various methods are given in the literature to implement virtual inertia. The derivative based control method is applied to provide virtual inertia through imitating the characteristics of a synchronous generator [10-12]. The H- $\infty$  based VIC minimizes the frequency fluctuations which causes due to wind and solar power variation [13]. While the effect of change in load on system frequency in case of low inertia system is mitigated through a fuzzy logic controller [14]. The model predictive controller based VIC maintains robustness of system during uncertainties over the derivative and fuzzy logic based VIC [15]. For deciding the gain of virtual inertia controller the eigenvalue sensitivity and parametric variation analysis is carried out [16, 17]. The RES must contain another source of generation to compensate its intermittent nature of input energy [18]. The fast reaction power resources such as BESS, flywheel, super-capacitor, SMES are used to provide inertial power in the system. The frequency nadir is influenced by the amount of power provided by fast responsive power storage resources. The factors need to consider for analysis of the performance of BESS based VI controller are the effects of weights in controller, effect of battery size, effect of time reaction [19]. The supercapacitor controls virtual inertia by maintaining the voltage references of super-capacitor according to the grid frequency variation [20]. A flywheel ESS is more advantageous than the batteries as it has higher power density and longer lifetime. Flywheel controls inertia by maintaining its speed proportional to frequency of grid [21]. The Superconducting Magnetic

Energy Storage (SMES) based VIC gives better performance in addition with less settling time than other storage systems [22]. The dynamic support through ESS to provide virtual inertia as frequency control ancillary services. It should comply with the requirements such as i) time of deployment ii) Duration of delivery iii) end of delivery [23]. The provision of VI is classified in two categories such as synchronously and synthetically. The inertial response achieves synchronously through rotating stabilizers, pumped hydro, wind turbines, gas turbine, diesel generator and synthetically such as battery technology, flywheels, HVDC interconnectors, Demand Side Response [24-26]. Employing the inertial response in RES dominated grids to curtail the high RoCoF propels the need for fast power injection. To provide this type of service the Fast Frequency Responses (FFR) are required to arrest frequency declination. The factors that need to be considered for coordinating the action of FFR are speed of response, the magnitude of response, control technique, repeatability, and availability of response [27-29]. It is necessary to emphasize the estimation of inertia value to provide an accurate inertial response. The state of art in the conventional swing equation-based estimation technique is enhancing the accuracy of estimation [30-32]. The demand response is introduced to mitigate the reduction in system inertia value [33]. An analysis of the contribution of demand-side inertia is done on previous frequency deviation events [34]. When inertia calculation is based on the power demand the contribution of inertia is in between 0.09s - 4.25s according to the category of consumer [35]. The various virtual inertia control topologies are analysed and classified in literature. After analysing various topologies/methodologies it is concluded that the best method suitable to provide a virtual response is based on the exact replication of synchronous generator response [36].

The contribution of this paper is listed as follows:

- The analysis of the effect of different generation mix is done on IEEE 9-bus system in power world simulator.
1. The performance of frequency response and inertia value of system is studied at different cases such as i. conventional system, ii. with solar power generation, iii. With solar and wind generation.
  2. The performance of frequency response and inertia value of system analysed at change in percentage wise share of RES in system.

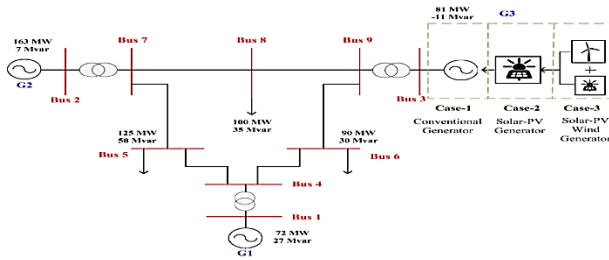


Fig. 1. IEEE 9 test bus system for analysis

This analysis gives the idea of response of system at low inertia values and this is motivation for proposed Modified Virtual inertia control.

- There are so many different methodologies are given in the literature to provide virtual inertia. There is lack of consideration of duration of inertial response and acceptable range of RoCoF. Due to this, the usage of resources that provides inertial response is operated more than the actual requirement. In this paper, the proposed modified virtual inertia control considers this factor while providing the inertial response.
- The proposed technique is compared with the system without VIC, with derivative based VIC, with fuzzy based VIC. The response of Modified-VIC is better among all these control topologies.
- The proposed topology is also analysed at different contingency event to check its robustness.

As aforementioned, the importance of inertia for frequency control ancillary services through PV generation is also another motivation of this paper.

## 1.2. Organization of paper

To implement the virtual inertia control it is necessary to investigate the effect of penetration of RES on frequency response and inertia value. It is investigated in section 2 at different scenarios and this analysis is done in power world simulator software. An importance of inertia in power system and factors affected in inertia constant value is explained in section 3. The section 4 elaborates the mathematical and dynamic modelling of single area system with solar PV generation. The modified virtual inertia controller in single area system is explained and implement in section 5. The simulation of PV generation in single area system is done in MATLAB Simulink and result analysis is presented in section 6. The requirement of inertia in power system and proposed VIC topology is concluded in section 7.

## 2. ANALYSIS OF FREQUENCY RESPONSE OF 9-BUS SYSTEM WITH PENETRATION OF RES

The large power systems with synchronous generators

are operate coherently and maintain the stable operation. The synchronous generators (rotor) are electrically coupled and share the load power. The controllable input sources in conventional generators regain the frequency stability after the disturbances or contingency events. The rotor rotates at synchronous speed which means at steady state condition the  $P_m = P_e$ . At the time of disturbances such as sudden load switch on/off or loss off generation etc. the  $P_m$  is not equal to  $P_e$ . The rotor accelerates and deaccelerates according to event and take some time to change the frequency due to mechanical inertia. This change in frequency ( $\Delta f$ ) signal goes to negative feedback system and generator changes its output power to feed the loss and maintain the frequency in acceptable range. The automatic load sharing capability of SG is govern by the frequency droop due to inverse proportionality between droop and generators. The small capacity generators have high droop gain and large capacity generators have low droop gain. The droop characteristic provides inherent load sharaing among the generators coupled parallely in electrical power system.

For flexible and reliable operation of power grid with high contribution of RES is need to accommodate the RES with frequency control mechanism like SG. To achieve this objective the analysis of performance of RES should be done at different conditions. To study this the IEEE 9-bus system is considered for the analysis purpose as shwon in figure 1. The different cases are considered such as,

Case 1: system with all synchronous generator,

Case 2: replacement of synchronous genertor with solar PV at bus 3,

Case 3: replacement of solar PV plus wind generation at bus 3.

The RoCoF and frequency nadir are the two primary metric of frequency stability analysis. Frequency nadir is dependent on the size of the contingency event and the inertial response of the generator. The RoCoF depends on the time required to respond to the power system disturbances and is measured in Hz/s. The RoCoF amplifies due to low mechanical inertia in the power system. There is a trade-off between frequency nadir, RoCoF, and inertial response. These factors should investigate at different operating conditions for developing the control topologies. The different scenarios are mentioned in Table 1 to study the frequency stability. The simulation study of the IEEE-9 bus system is carried out in power world simulator software to justify this problem.

**Table 1. Different scenarios used to study the effect of RES in power system frequency stability**

Case	Scenarios under study
Case A	System with synchronous generators
Case B	System with synchronous generators replaced by solar power generation
Case C	System with synchronous generators replaced by solar + wind power generation
Case D	System with percentage-wise rise in solar power generation
Case E	Study of effect of rise in load with equal contribution of RES

To study the frequency response, the generated disturbance is 10% rise in load from 3 to 4 seconds at bus number 5.

**Case A:** Figure 2 depicts the performance of frequency response with conventional generators. Due to disturbance, the frequency nadir point reaches 49.832 Hz at 4.485 seconds. The table 3 and 4 are elaborate on the frequency response analysis with a rise in load up to 40%. It is observed from the simulation result analysis given in table 3, the size of contingency affects the frequency nadir point in the conventional generator. RoCoF is not that considerable due to the constant inertia available in a synchronous generator.

**Case B:** The conventional generator connected to bus number 3 is replaced by the solar PV generator. The solar PV generator is entirely static; it does not contain inertia. The simulation results in figure 3 show the frequency nadir is 49.771 Hz at 3.09 sec. Compared to “case A,” the time taken to reach the nadir point is reduced by 31.10 %. **Case B** represents the inertia-less system is more vulnerable to power system disturbances. Tables 3 and 4 depict the further analysis of the effect of a percentage-wise increase in load on frequency nadir and RoCoF.

**Case C:** The 9-bus system incorporated with penetration of solar PV plus wind at bus number 3. The system with wind generation has a frequency nadir 49.802 Hz at 3.09s depicted in figure 4. The nadir point is improved by 0.031Hz compared to “case B.” Due to the presence of the turbine, the wind power generator has some inertia. The simulation results concluded that the inertia value varies according to the type of generator mix.

**Case D:** The frequency response and inertia constant were analyzed by increasing the percentage-wise share of solar PV in the 9-bus test system. The RES percentage is calculated as follows:

$$RES(\%) = \frac{RES \text{ penetration}(MW)}{Total \text{ Generation}(MW)} * 100 \tag{1}$$

The inertia constant becomes a heterogeneous quantity with an increase in the share of solar PV

generators. It is calculated from the equation of RoCoF given as:

$$RoCoF = \frac{f_0 * \Delta P}{2 * H_i * S_i} \tag{2}$$

Where  $f_0$  is the nominal frequency and  $\Delta P$  is the change in active power,  $H_i$  and  $S_i$  are the inertia constant and system base. It is observed from Table 2; the inertia constant is reduced by 1.8856s when the contribution of solar PV generation reaches 50%. According to this analysis, the grid operator should consider the decay in inertia value for further corrective action.

**Case E:** The frequency response analysis at a percentage-wise increase in load is done at three different scenarios. Naturally, the increase in load causes a frequency drop. The decline in frequency depends on the type of generation mix that participated in providing an inertial response. This comparison is shown in Tables 3 and 4, respectively. The frequency nadir and RoCoF increases with an equal share of solar for the same contingency event. When wind power generation comes into the picture, there is a slight improvement in nadir and RoCoF.

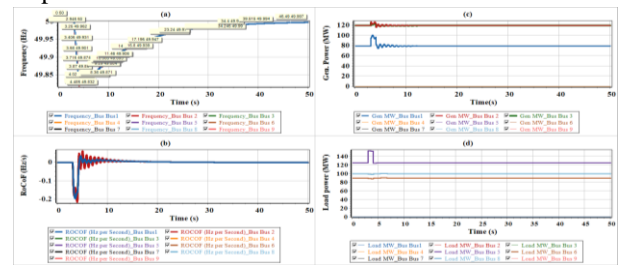


**Fig. 2. Performance of system with conventional generators (a) Frequency response, (b) RoCoF, (c) Generator power (MW) and (d) load power (MW)**

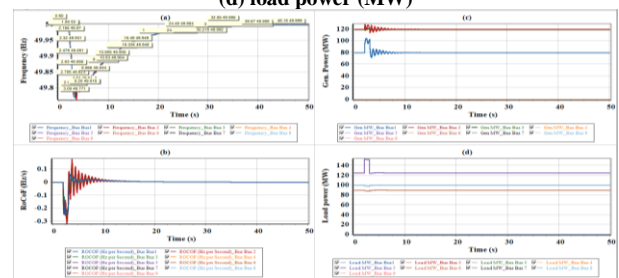


**Fig. 3. Performance of system with contribution of solar PV - (a) Frequency response, (b) RoCoF, (c) Generator power (MW) and (d) load power (MW)**

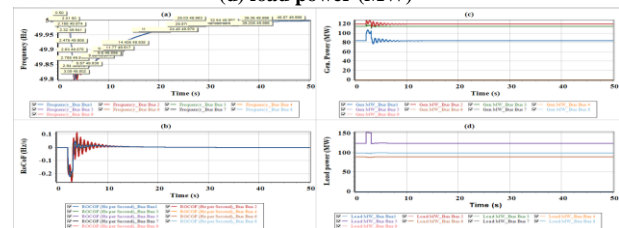


**Fig. 4. Performance of system with contribution of solar PV and wind generator - (a) Frequency response, (b) RoCoF, (c) Generator power (MW) (d) load power**

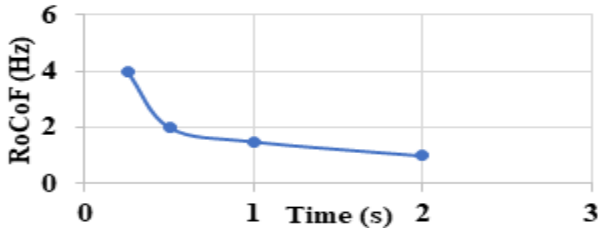


Fig. 6. The time required to reach frequency nadir at RoCoF

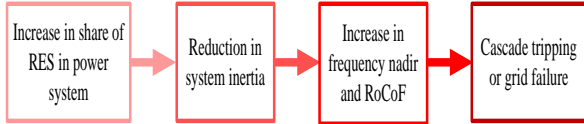


Fig. 5. Impact of inertia due to large penetration of RES

### 3. IMPORTANCE OF INERTIA IN THE POWER SYSTEM

Challenges in Renewable Energy Sources (RES) integrated power systems are stability, adequacy, and flexibility. For stable system operation, it is necessary to maintain the supply and demand balance. A rigid power system keeps the frequency in range after a contingency event. The presence of inertia in the power system

reduces frequency dynamics. The power system with adequate inertia is less responsive to minor disturbances. The KE stored in the rotor of the synchronous contributes to inertia. The system's analysis with RES and the frequency response at different scenarios show the requirement of virtual inertia in future power systems. The RES's are integrating with the grid through a power electronic converter. These converter-based generators rapidly respond to any change due to the absence of rotating or mechanical parts. The low inertia systems create frequency instability issues, which need the development of new frequency control techniques. Figure 5, describes the events after high-RES share in power grids. Low inertia systems are susceptible to minor disturbances. Due to the decaying of the RoCoF hence generation frequency is unable to come in the operating range and results in cascade tripping or blackout. The concrete solution is the synthetic inertia provision by following frequency dynamics for this problem. These two points are discussed with their detailed study in the following sections.

Table 2. Values of frequency nadir, RoCoF and inertia at increase in percentage share of solar

	Share of solar (%)														
	10%			20%			30%			40%			50%		
	Frequency (Hz)	RoCoF (Hz/s)	Inertia (H(S))	Frequency (Hz)	RoCoF (Hz/s)	Inertia (H(S))	Frequency (Hz)	RoCoF (Hz/s)	Inertia (H(S))	Frequency (Hz)	RoCoF (Hz/s)	Inertia (H(S))	Frequency (Hz)	RoCoF (Hz/s)	Inertia (H(S))
Bus 1	49.8	-0.221	3.5	49.786	-0.237	3.2700	49.77	-0.253	3.0632	49.744	-0.342	2.2660	49.714	-0.411	1.8856
Bus 2	49.797	-0.243	3.1	49.783	-0.276	2.8079	49.763	-0.318	2.4371	49.738	-0.375	2.0666	49.721	-0.453	1.7108
Bus 3	49.799	-0.255	3.0392	49.787	-0.265	3.0273	49.772	-0.302	2.5662	49.747	-0.352	2.2017	49.722	-0.414	1.8719
Bus 4	49.802	-0.217	3.5714	49.789	-0.228	3.3991	49.775	-0.243	3.1893	49.75	-0.277	2.7998	49.717	-0.323	2.3993
Bus 5	49.802	-0.212	3.6556	49.789	-0.234	3.3119	49.775	-0.262	2.9580	49.752	-0.303	2.5577	49.72	-0.357	2.1708
Bus 6	49.802	-0.224	3.4598	49.789	-0.234	3.3119	49.775	-0.26	2.9807	49.752	-0.299	2.5919	49.72	-0.35	2.2142
Bus 7	49.799	-0.228	3.3991	49.786	-0.261	2.9693	49.765	-0.3	2.5833	49.743	-0.353	2.1954	49.724	-0.422	1.8364
Bus 8	49.8	-0.228	3.3991	49.786	-0.258	3.0038	49.77	-0.296	2.6182	49.746	-0.348	2.2270	49.724	-0.414	1.8719
Bus 9	49.801	-0.237	3.2700	49.787	-0.257	3.0155	49.77	-0.293	2.6450	49.749	-0.342	2.2660	49.729	-0.402	1.9278

Table 3. Frequency nadir at percentage change in load with contribution of solar and solar +wind in 9 bus system

	Frequency (Hz) at Change in load (%)											
	10%			20%			30%			40%		
	Conventional gen	With solar	With solar + wind	Conventional gen	With solar	With solar + wind	Conventional gen	With solar	With solar + wind	Conventional gen	With solar	With solar + wind
Bus 1	49.82	49.799	49.812	49.658	49.611	49.635	49.504	49.436	49.47	49.362	49.274	49.318
Bus 2	49.817	49.796	49.808	49.65	49.605	49.627	49.493	49.426	49.458	49.347	49.261	49.301
Bus 3	49.82	49.799	49.811	49.657	49.611	49.634	49.503	49.436	49.468	49.36	49.274	49.314
Bus 4	49.821	49.801	49.813	49.659	49.615	49.638	49.505	49.441	49.475	49.364	49.281	49.324
Bus 5	49.821	49.801	49.812	49.658	49.614	49.636	49.503	49.44	49.471	49.361	49.279	49.319
Bus 6	49.821	49.802	49.813	49.659	49.615	49.638	49.506	49.442	49.474	49.364	49.282	49.322
Bus 7	49.818	49.798	49.809	49.653	49.608	49.63	49.497	49.432	49.463	49.353	49.268	49.308
Bus 8	49.819	49.799	49.81	49.655	49.61	49.632	49.5	49.434	49.465	49.356	49.271	49.311
Bus 9	49.82	49.80	49.811	49.657	49.612	49.634	49.503	49.437	49.468	49.36	49.276	49.315

**Table 4. RoCoF at percentage change in load with contribution of solar and wind + solar in 9 bus system**

	RoCoF (Hz/s) at Change in load (%)											
	10%			20%			30%			40%		
	Conventional gen	With solar	With solar + wind	Conventional gen	With solar	With solar + wind	Conventional gen	With solar	With solar + wind	Conventional gen	With solar	With solar + wind
Bus 1	-0.198	-0.223	-0.21	-0.378	-0.433	-0.407	-0.548	-0.628	-0.591	-0.705	-0.808	-0.76
Bus 2	-0.217	-0.242	-0.235	-0.413	-0.467	-0.455	-0.598	-0.676	-0.658	-0.767	-0.869	-0.847
Bus 3	-0.202	-0.247	-0.229	-0.385	-0.479	-0.444	-0.556	-0.696	-0.642	-0.711	-0.9	-0.824
Bus 4	-0.185	-0.218	-0.201	-0.352	-0.422	-0.389	-0.511	-0.614	-0.565	-0.658	-0.79	-0.727
Bus 5	-0.186	-0.213	-0.201	-0.354	-0.411	-0.39	-0.512	-0.595	-0.563	-0.656	-0.763	-0.723
Bus 6	-0.185	-0.222	-0.201	-0.352	-0.431	-0.388	-0.509	-0.626	-0.562	-0.651	-0.808	-0.724
Bus 7	-0.206	-0.229	-0.225	-0.393	-0.442	-0.436	-0.568	-0.64	-0.631	-0.729	-0.821	-0.811
Bus 8	-0.203	-0.228	-0.224	-0.387	-0.441	-0.434	-0.559	-0.637	-0.628	-0.717	-0.818	-0.807
Bus 9	-0.199	-0.231	-0.223	-0.379	-0.448	-0.431	-0.547	-0.652	-0.624	-0.701	-0.842	-0.801

### 3.1. Rate of Change of Frequency (RoCoF)

The RoCoF is the primary metric to determine the frequency stability. RoCoF is directly affected by the amount of inertia present in the system. It requires a substantial perturbation of load to violate the generation and demand balance in large grids. The high stiffness constant required to cause a change of 1Hz in frequency. For a vast power grid with a high share of conventional generators, the RoCoF (df/dt) is less. Therefore, large-sized grids are rigid to rapid frequency fluctuations during load perturbations. For continuous and large load perturbations, the frequency goes below the threshold value that causes tripping of generators. So, it is essential to know the RoCoF for initiating the corresponding actions to maintain the expected frequency range. The lower RoCoF increases the time to reach the frequency nadir value. Figure 6 represents the relationship between the time required to get the minimum frequency point at different RoCoF.

### 3.2. Inertial response in the conventional system

The inertial response is based on the system's stored KE ( $E_{kinetic}$ ). Where,

$$E_{kinetic} = \frac{1}{2} J \omega^2 \quad (3)$$

The  $J$  denotes the moment of rotor inertia in ( $kg \cdot m^2$ ), and  $\omega$  is the synchronous speed in  $rad/sec$ . Inertia constant is described as the ratio of kinetic energy ( $E_{kinetic}$ ) stored in the generator rotor, which is in mega joules to the rating of the machine (S) in MVA.

$$H = \frac{E_{kinetic}}{S} \quad (4)$$

The generated power is fixed-parameter in conventional generators, while the connected load is variable. The dynamic modelling of the component such as generator, turbine, and load damping block is done to analyse the effect of the load change on the power system frequency.

## 4. MATHEMATICAL AND DYNAMIC MODELLING OF PV GENERATION IN SINGLE-AREA SYSTEM

The total power must be zero for the stable operation when consumption equals the generation. Practically there is always a gap between demand and supply as the load is the variable quantity for the dynamic analysis of the power system. Whenever there is a load change, it causes the contradiction in mechanical and electrical input power, resulting in the variation in speed as determined by the equation of motion. A small perturbation in the system causes a change in angular velocity ( $\Delta\omega$ ), leading to the deviation in system frequency ( $\Delta f$ ), as shown in figure 7.

Where  $\Delta P_m$  is change in mechanical power,  $\Delta P_e$  is changed in electrical power,  $\Delta f$  changes in frequency,  $H$  is inertia constant, and  $s$  is Laplace operator.

The power systems loads are composite of frequency-dependent and frequency-independent loads. The comprehensive characterization of mixed loads is expressed as

$$\Delta P_e = \Delta P_L + D \Delta \omega \quad (5)$$

Where  $\Delta P_L$  is a change in load power,  $\Delta \omega$  represents a change in angular speed, and  $D$  is the load-damping constant. The damping constant means the percent change in load to the frequency. Figure 7(b) shows the effect of load damping and block reduction in figure 7(c).

The inertia constant determines the system response to the load change in the absence of speed governor action. The dynamic model of a single area system with thermal power generation is given in figure 8. The droop governor action tunes the generator output ( $\Delta P_m$ ) in frequency regulation. The simple first-order function is used for modeling governor action.

$$\Delta P_G = \Delta P_{ref} - \frac{1}{R} \Delta f \tag{6}$$

$$\Delta P_m = \frac{1}{1 + T_i s} \Delta P_G \tag{7}$$

$$ACE = \frac{K}{s} (\beta \cdot \Delta f) \tag{8}$$

Where,  $\Delta P_{ref}$  determines the set point of reference power,  $T_i$  is turbine time constant, and  $\Delta P_G$  is input signal for the governor-turbine action.

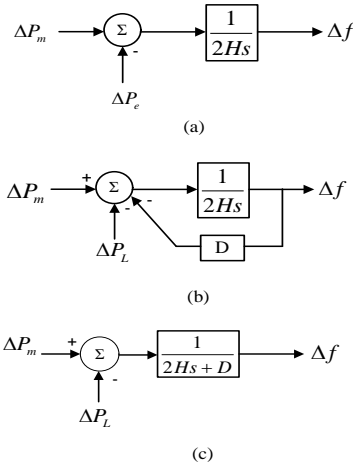


**Fig. 7. Load damping model (a) transfer function relating speed and power (b) effect of load damping (c) inertia constant and damping constant**

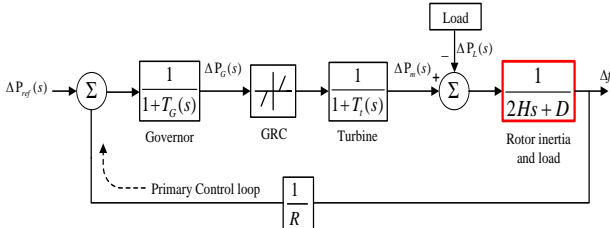


**Fig. 8. Dynamic Modelling of single-area system**

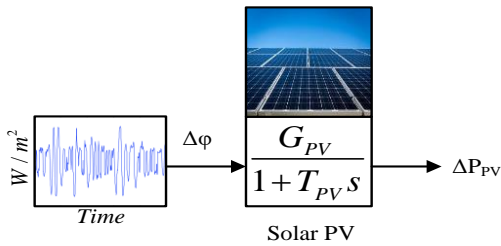


**Fig. 9. A dynamic model of solar PV**

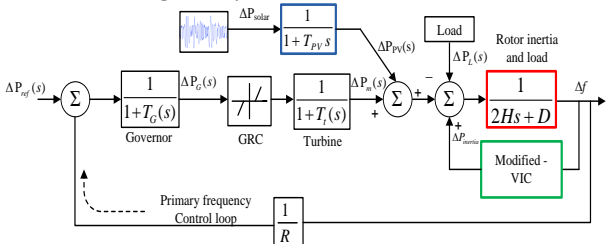


**Fig. 10. Solar PV generation in single area system with Modified-VIC**

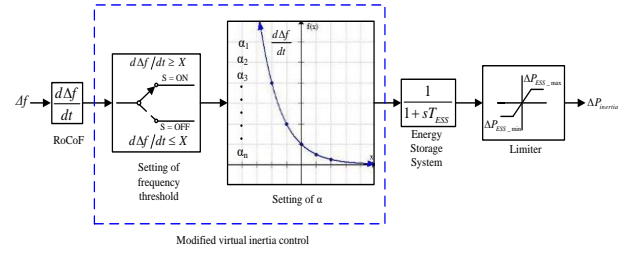


**Fig. 11. Modified-VI Controller (M-VIC)**

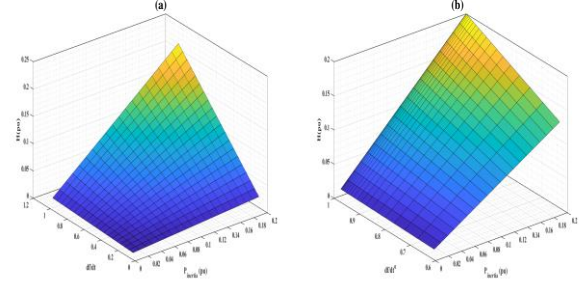


**Fig. 12. Virtual inertia coefficient versus  $df/dt$  and  $\Delta P_{inertia}$  (a) Virtual inertia in conventional VIC (b) Virtual inertia in M-VIC**

In this paper, the model of a single area with a solar PV generator is considered for VIC emulation. As there is variability in input power, solar PV generator characteristics are different from conventional generators. The power electronic converters have a minimal time constant compared to the synchronous generators mechanical time constant. While considering this issue, the response time to the disturbance in the power system is different in both synchronous and Solar PV generators. However, the solar power input is not constant; therefore, it also creates disturbances in the power system. The Dynamic modeling of the solar system is stated below:

The nature of solar power input/energy fluctuates while considering this phenomenon; the following model is given. However, the overall dynamics of the solar power plant are not considered as it increased the order of the system. Figure 9 shows the lower-order linearized model of the solar PV is taken for the assessment of frequency response in a single area system. The first-order transfer function of solar model imitates the overall time response of solar PV system Ref. [37]. The input to the solar power plant is a change in irradiance ( $\Delta$ ) with respect to time [38]. For realizing the effect of a grid-integrated solar power plant, the PV output power is determined by equation (9).

$$P_{PV} = \eta S \phi (1 - 0.005(T_a + 25)) \tag{9}$$

Where,  $\eta$  is conversion efficiency which is between 8% to 15%,  $S$  is PV array area in ( $m^2$ ),  $\phi$  is irradiance in ( $W/m^2$ ) and,  $T_a$  is Ambient temperature ( $^{\circ}C$ );

The efficiency of conversion ( $\eta$ ) and area of PV

array ( $S$ ) are constant; therefore, the PV output power depends on ambient temperature ( $T_a$ ) and irradiance ( $\phi$ ). The solar PV system dynamic modelling consists of the equation (10). Where  $T_1$  and  $T_2$  are the time constant of the converter respectively.

$$\frac{1}{1+T_1(s)} \times \frac{1}{1+T_2(s)} = \frac{1}{1+(T_1+T_2)s+T_1T_2s^2} \cong \frac{1}{1+T_c(s)} \quad (10)$$

The generalized first-order transfer function of the solar PV for the dynamic analysis is given in equation 11. In the first-order transfer function of the solar PV system, the time constant is represented as  $T_{PV}$  for the dynamic analysis of the power system.

$$K_{PV} = \frac{1}{1+T_{PV}(s)} = \frac{\Delta P_{PV}}{\Delta P_{solar}} \quad (11)$$

Where,  $K_{PV}$  is the Ratio of change in power ( $\Delta P_{PV}$ ) to the change in solar power ( $\Delta P_{solar}$ ) due to change in irradiance ( $\Delta \phi$ ). The of single area system with PV generation and virtual inertia control is represented in figure 10.

The lower order dynamic model of a single area with solar PV generation is

$$\Delta f = \frac{1}{2Hs + D} (\Delta P_{PV} + \Delta P_{inertia} + \Delta P_m - \Delta P_L) \quad (12)$$

### 5. MODIFIED VIRTUAL INERTIA CONTROL (M-VIC)

In synchronous generators, stored KE is proportional to system inertia. At the time of any frequency event, the rotor releases its stored energy and prevents the system from low-frequency nadir. The value of virtual inertia constant can be adjusted flexibly. The too-small value of the inertia coefficient increases the frequency nadir, and the too-large value of inertia causes higher frequency overshoot and oscillations. This must be considered while designing the VIC. The magnitude and duration of the disturbances are not considered in derivative-based VIC; it is taking action by following the  $(d\Delta f/dt)$  signal. However, the active power setpoint continuously switches in line with the frequency change rate. The ESS provides active power for the virtual inertial response. It is not advisable to change the set point of active power at every instant; due to its charging and discharging limitations. There is no need to change the inertial response in steady-state grid operation. This factor is considered in the modified virtual VI controller. The threshold value of frequency change rate or RoCoF is set in M-VIC. The proposed

method avoids the false RoCoF triggering. The inertia coefficient is maintained dynamically in the proposed M-VIC. The use of the threshold  $X$  prevents frequent and unnecessary utilization of energy storage systems. The inertia coefficient is adapted according to the contingency event's severity and the disturbance's duration. A higher inertial response is selected at a contingency to reduce the frequency nadir point. After the disturbance, the ESS stops providing active power input ( $\Delta P_{inertia}$ ) to avoid power oscillations when the system reaches steady-state operation. The proposed control technique emulates the inertial power according to the severity of the RoCoF ( $d\Delta f/dt$ ) by adapting the factor ( $\alpha$ ). The relationship between  $\Delta P_{inertia}$  and the  $(d\Delta f/dt)$  is inversely proportional; as shown below,

$$H_{VI} = \frac{\Delta P_{ESS\_max}}{(d\Delta f / dt)^\alpha} \quad (13)$$

The exponential term ( $\alpha$ ) selection depends on  $(d\Delta f/dt)$ 's decaying rate. The exponential term ( $\alpha$ ) emulates the rate at which the deficit of inertial power requirement can be fulfilled. The function actuates when it exceeds a threshold of RoCoF. The threshold value is set as the acceptable limits of the frequency change rate at a steady state. In the proposed control, the inertia ( $H_{virtual}$ ) change times are reduced by setting  $X$ . The exponential term ( $\alpha$ ) helps to overcome the frequency decay due to disturbance. The proposed Modified-VIC is presented in figure 11.

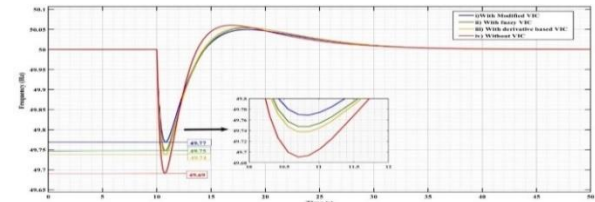


Fig. 13. Comparison of frequency responses of system i) without M-VIC, ii) with fuzzy VIC, iii) with derivative VIC, iv) without VIC

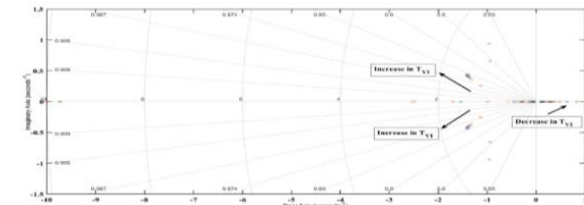


Fig. 14. Pole-zero map at various values of energy storage system time constant ( $T_{VI}$ )

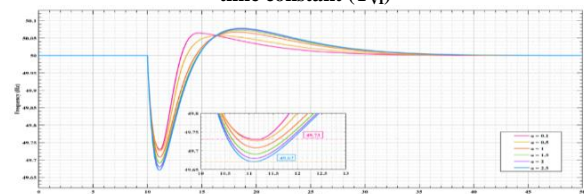


Fig. 15. Effect of different values of factor  $\alpha$  on frequency response

**Table 5. Comparison of frequency nadir and RoCoF at different VIC**

Control	Frequency Nadir (Hz)	RoCoF (Hz/s)
Without VIC	49.69	0.4428
With derivative-based VIC	49.74	0.3714
With fuzzy based VIC	49.75	0.3571
M-VIC	49.77	0.3285

**Table 6. Frequency nadir and RoCoF at disturbances in system**

Control	Disturbance in solar power input		Load disturbance	
	Frequency Nadir (Hz)	RoCoF (Hz/s)	Frequency Nadir (Hz)	RoCoF (Hz/s)
Without VI control	49.5983	0.1908	49.7014	0.174
With VI control (derivative-based)	49.6433	0.1626	49.7367	0.15
Modified VI control	49.6909	0.1350	49.7748	0.12

Figure 12 displays the 3-dimensional plots to depict the performance of the virtual inertia ( $H_{virtual}$ ) in conventional VI control in (a) and modified VI control in (b). The growth rate of virtual inertia ( $H_{virtual}$ ) is increased in the modified VI controller. The exponential factor ( $\alpha$ ) is contributed to enhancing the increasing rate of VI according to the size of disturbance.

## 6. SIMULATION RESULTS AND DISCUSSIONS

### 6.1. System configuration

This paper focuses on the single area system with solar PV generation, including 15 MW of composite loads, 8 MW and 7 MW of thermal generation, and solar PV generation, respectively. The 3 MW of ESS is used to provide inertial power. The dynamic model of the system is represented in figure 10.

### 6.2. Simulation result studies

The system with modified VI control shows a significant difference in frequency nadir point and setting time compared to without VI control. The M-VIC is compared with other VIC topologies such as derivative-based and Fuzzy VIC; it is presented in figure 13. The derivative-based VIC uses  $\Delta f$  signal value for taking corrective action. In fuzzy-based VIC, the  $\Delta f$  and  $\Delta PPV$ , these two inputs are taken for making fuzzy rules. It is observed from figure 13, the frequency nadir at system with:

- i. Modified VIC is 49.77Hz.
- ii. Fuzzy-based VIC is 49.75Hz.
- iii. Derivative-based VIC is 49.74 Hz.
- iv. Without VIC is 49.69Hz.

The M-VIC gives better performance compared to fuzzy and derivative-based VIC. There is a very slight difference of 0.01 Hz in frequency nadir value of fuzzy and derivative VIC. Due to this reason, the fuzzy VIC is not considered for further

comparative analysis at different power system scenarios. The RoCoF is also improved in the proposed control technique and the observation of frequency response at different controls is compared in Table 5. The time constant ( $T_{VI}$ ) of the converter-based ESS plays a vital role in the stability of the modern grid. The pole-zero map of the same is shown in figure 14. The less  $T_{VI}$  ruptures the stability of the power system for the stable operation, the range of  $T_{VI}$  is between 5-10.

The inertial power in the proposed topology is mentioned equation (13), and the term  $\alpha$  is selected empirically. The selection of  $\alpha$  is depended on the severity of the RoCoF. The lower values of  $\alpha$  give better frequency nadir. According to this observation, at the time of disturbances, the lower values of  $\alpha$  are selected for providing a higher inertial response. Figure 15 depicts the effect of variation in factor  $\alpha$  on frequency nadir.

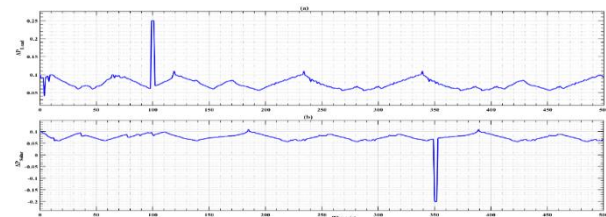


**Fig. 16. Variation in Solar Power and Load power**

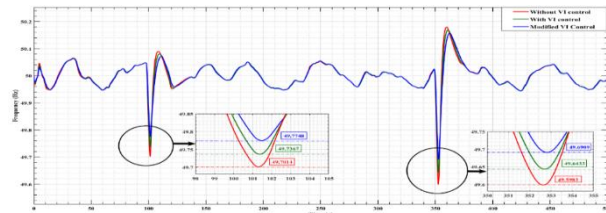


**Fig. 17. Frequency response without VI control, With VI control, With modified VI control**

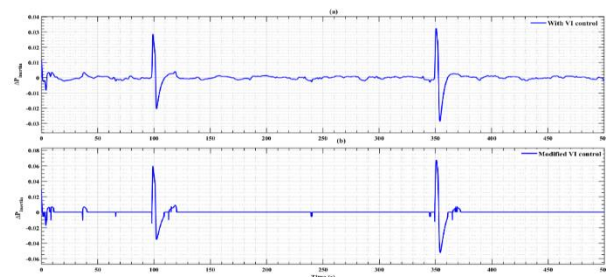


**Fig. 18. Inertial Power ( $\Delta P_{inertia}$ )**

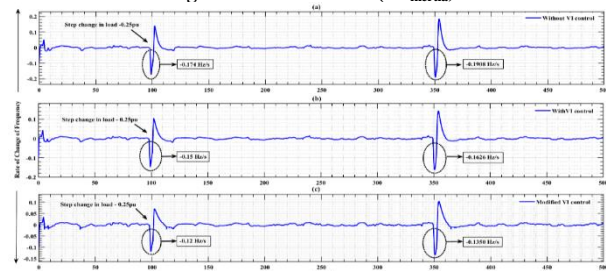


**Fig. 19. Rate of Change of Frequency**

Simulation results study accommodates the single area system with conventional and PV generation

systems. For analyzing the performance of the modified VI control, the disturbances are created at 100s and 350s, respectively as shown in figure 16. At 100s and 350s, a sudden increase in load by 25% and a change in solar input by 40% is represented in figure 16.

The situations of abrupt load change and deviation in solar power input and their effect on frequency response at different virtual inertia controllers are displayed in figure 17. The modified VI controller improves the frequency response at disturbance situations. The analysis of frequency response at disturbances is given in table 6.

The proposed control technique meliorates the inertial power response and requisite the utilization of an energy storage system. It is not considered in derivative-based VI control. The proposed modified-VI controller is designed based on these two factors: i) the charging and discharging limitations of ESS, ii) the acceptable frequency band given by Electricity Regularity Authorities. When RoCoF is in an acceptable range, then practically, there is no need for inertial power in the system. The  $\Delta P_{inertia}$  provided by conventional VI control and modified VI control is depicted in figure 18. The proposed technique works only when inertial power is required. The power system stability is very vulnerable to the RoCoF. The extensive penetration of renewable sources creates high RoCoF at the small perturbation of load. Figure 19 illustrates the performance of RoCoF. It is observed in figure 19(a), for a step-change in load by 0.25pu, the RoCoF at the system without VIC is 0.174Hz/s. Similarly, for derivative-based VIC and M-VIC, the RoCoF are 0.15Hz/s and 0.12Hz/s, respectively. Hence, the simulation studies assure that the modified VI-controller enhances the firmness of the system response under different contingencies.

## 7. CONCLUSION

The analysis of power system frequency response with increase in share of RES (solar PV and wind) is done on IEEE 9-bus test system. It is very necessary to understand the response of RES in generation mix to design the appropriate topology for frequency regulation. The effect of rise in RES on frequency nadir, RoCoF and inertia value is verified in 9-bus system. As the share of solar increases from 10% to 50% the value of inertia constant at bus 1 is degraded from 3.5s to 1.8856s respectively. The effect of load disturbances on frequency response in generation mix system is varied according to the type of resources are present in the system. As rise in load from 10% to 40% at different generation mix scenario is varied according to

availability of amount of inertia. The change in frequency nadir at 10% change in load for different cases: i. Only with conventional generation, ii. With solar, iii. With solar and wind is 49.82Hz, 49.799Hz, 49.812Hz respectively at bus1. This shows for same percentage change in load the frequency nadir point is higher in case of solar generation. The RoCoF at 10% change in load at i. Only with conventional generation, ii. With solar, iii. With solar and wind is -0.198 Hz/s, -0.223 Hz/s, -0.21Hz/s, respectively. This shows RoCoF is higher in system with solar generation because of low inertia constant. This paper has proposed a modified virtual inertia controller for the enhancement of the frequency response in grid integrated PV generation system. In the proposed control topology, the VI emulated by controlling the rate of active power provision from the external ESS. The proposed control topology effectively improves the frequency nadir and RoCoF compared with derivative based and fuzzy VIC. In addition, the proposed control also take care about the proper utilization of the ESS which is not considered in previous control topologies. The M-VIC regulates virtual inertia ( $H_{virtual}$ ) dynamically.

The presented work in this paper motivates the integration of renewable energy sources in the power grid. The objective of this work is the virtual inertia as an ancillary service (frequency control) in RES integrated grid is fulfilled.

## Appendix A.

Damping constant,  $D$  (pu. MW/Hz) = 0.016, Droop constant,  $R$  (Hz/p.u.MW) = 2.4, Inertia Constant,  $H$  (pu. MWs) = 0.5, Time constant of governor,  $T_g$ (s) = 0.1, Time constant of turbine,  $T_t$ (s) = 0.4, Virtual Inertia control gain(derivative-based),  $K_{VI}$  (s) = 0.5, Virtual Inertia time constant,  $TVI$  (s) = 5, Solar PV system time constant,  $TPV$ (s) = 0.5, Solar PV system gain,  $K_{PV}$ (s) = 1.

## REFERENCES

- [1] M. Allahnoori et al., "Reliability assessment of distribution systems in presence of microgrids considering uncertainty in generation and load demand", *J. Oper. Autom. Power Eng.*, vol. 2, pp. 113-120, 2014.
- [2] T. Kerdphol, F. Rahman, and Y. Mitani, "Virtual inertia control application to enhance frequency stability of interconnected power systems with high renewable energy penetration", *Energies*, vol. 11, pp. 981, 2018.
- [3] A. Ulbig, T. Borsche, and G. Andersson, "Impact of low rotational inertia on power system stability and operation", *IFAC Proc. Vol.*, vol.47, pp.7290-7,2014.
- [4] Task force members from REE, T., TransnetBW, 50Hertz and R. Transmission, Swissgrid and Energinet.dk., Frequency Stability Evaluation Criteria for the Synchronous Zone of Continental Europe, Report of

- European network of Transmission system operators for electricity, pp. 1-25, 2016.
- [5] Commission, C.E.R., Grid Security Need for Tightening of Frequency Band & Other Measures.
- [6] AISBL, E.-E.E.-E., ENTSO-E draft network code for requirements for grid connection applicable to all generators. Brussels, Belgium, 2012.
- [7] H. Nerkar, P. Kundu and A. Choudhury, "Frequency control ancillary services in power system with integration of PV generation", *Int. Conf. Intell. Tech.*, pp. 1-6, 2021.
- [8] P. Tielens, and D. Van Hertem, "Grid inertia and frequency control in power systems with high penetration of renewables", *Young Res. Symp. Electr. Power Eng.*, 2012.
- [9] B. Mohammadi-Ivatloo et al., "An improved under-frequency load shedding scheme in distribution networks with distributed generation", *J. Oper. Autom. Power Eng.*, vol.2, pp. 22-31, 2014.
- [10] T. Kerdphol et al., "Demonstration of virtual inertia emulation using energy storage systems to support community-based high renewable energy penetration", *IEEE Global Humanitarian Tech. Conf.*, 2018.
- [11] P. Saxena, N. Singh, and A. Pandey, "Enhancing the dynamic performance of microgrid using derivative controlled solar and energy storage based virtual inertia system", *J. Energy Storage*, vol.31, pp. 101613. 2020.
- [12] N. Babu, B. Maddila, G. Panda, "Frequency stability enhancement of thermal power plant-integrated microgrid with virtual inertia emulation", *3rd Int. Conf. Energy Power Environ. Towards Clean Energy Tech.*, 2021.
- [13] T. Kerdphol et al., "Robust virtual inertia control of an islanded microgrid considering high penetration of renewable energy", *IEEE Access*, vol. 6, pp. 625-36, 2017.
- [14] K. Menteshidi et al., "Implementation of a fuzzy logic controller for virtual inertia emulation", *Int. Symp. Smart Electr. Distrib. Syst. Tech.*, 2015.
- [15] T. Kerdphol et al., "Virtual inertia control-based model predictive control for microgrid frequency stabilization considering high renewable energy integration", *Sustain.*, vol.9, pp.773, 2017.
- [16] E. Rakhshani et al., "Frequency control of HVDC interconnected system considering derivative based inertia emulation", *IEEE Power Energy Soc. Gen. Meet.*, 2016.
- [17] E. Rakhshani et al., "Analysis of derivative control based virtual inertia in multi-area high-voltage direct current interconnected power systems", *IET Gener. Transm. Distrib.*, vol. 10, pp.1458-69, 2016.
- [18] M. Hassas, K. Pourhossein, "Control and management of hybrid renewable energy systems: review and comparison of methods", *J. Oper. Autom. Power Eng.*, vol. 5, pp.131-138, 2017.
- [19] L. Toma et al., "On the virtual inertia provision by BESS in low inertia power systems", *IEEE Int. Energy Conf.*, 2018.
- [20] R. Zhang, J. Fang, and Y. Tang, "Inertia emulation through supercapacitor energy storage systems", *10th Int. Conf. Power Electron. ECCE Asia*, 2019.
- [21] J. Yu, J. Fang, and Y. Tang, "Inertia emulation by flywheel energy storage system for improved frequency regulation", *IEEE 4th South. Power Electron. Conf.*, 2018.
- [22] T. Kerdphol et al., "Applying virtual inertia control topology to SMES system for frequency stability improvement of low-inertia microgrids driven by high renewables", *Energies*, vol. 12, pp.3902, 2019.
- [23] G. Delille, B. Francois, and G. Malarange, "Dynamic frequency control support by energy storage to reduce the impact of wind and solar generation on isolated power system's inertia", *IEEE Trans. Sustain. Energy*, vol. 3, pp.931-9, 2012.
- [24] O. Konstantin et al., "Innovation in the Power Systems industry", *Cigre Science Eng.*, vol.11, pp.3-126, 2018.
- [25] H. Radmanesh, M. Saeidi, "Stabilizing microgrid frequency by linear controller design to increase dynamic response of diesel generator frequency control loop", *J. Oper. Autom. Power Eng.*, vol. 7, pp. 216-226, 2019.
- [26] K. Matsuda et al., "Stabilization of power system by virtual inertia control of adjustable speed synchronous condenser", *2nd Int. Conf. Rob. Electr. Signal Proc. Tech.*, 2021.
- [27] Fast frequency response concepts and bulk power system reliability needs, *NERC Report*, pp. 1-23, 2020.
- [28] G. Rietveld et al., "Evaluation report on the problem of rocof measurement in the context of actual use cases and the "wish list" of accuracy and latency from an end-user point of view", *EURAMET*, 2019.
- [29] R. Eriksson, N. Modig, and K. Elkington, "Synthetic inertia versus fast frequency response: a definition", *IET Renew. Power Gener.*, vol. 12, pp. 507-514, 2017.
- [30] C. Phurailatpam et al., "Measurement based estimation of inertia in AC microgrids", *IEEE Trans. Sustain. Energy*, 2019.
- [31] Y. Zhang et al., "Synchrophasor measurement-based wind plant inertia estimation", *IEEE Green Tech. Conf.*, 2013.
- [32] O. Beltran et al., "Inertia estimation of wind power plants based on the swing equation and phasor measurement units", *Appl. Sci.*, vol. 8, pp. 2413, 2018.
- [33] M. Rampokanyo, and P. Ijumba-Kamera, "Power system inertia in an inverter-dominated network", *J. Energy South. Africa*, vol. 30, pp. 80-86, 2019.
- [34] Y. Bian et al., "Demand side contributions for system inertia in the GB power system", *IEEE Trans. Power Syst.*, vol. 33, pp. 3521-30, 2017.
- [35] H. Thiesen, and C. Jauch, "Determining the load inertia contribution from different power consumer groups", *Energies*, vol.13, pp.1588, 2020.
- [36] U. Tamrakar et al., "Virtual inertia: current trends and future directions", *Appl. Sci.*, vol. 7, pp. 654, 2017.
- [37] D. Lee, and L. Wang, "Small-signal stability analysis of an autonomous hybrid renewable energy power generation/energy storage system part I: Time-domain simulations", *IEEE Trans. Energy Conv.*, vol. 23, pp. 311-20, 2008.
- [38] P. Rajendran, and H. Smith, "Modelling of solar irradiance and daylight duration for solar powered UAV sizing", *Energy Explor. Exploit.*, vol. 34, pp.235-43, 2016.